

Fluctuation Conductivity of Polycrystalline $Y_{1-x}Pr_xBa_2Cu_3O_{7-\delta}$ Superconductors

Alcione Roberto Jurelo*, Celmir Lupack de Araújo, Ezequiel Costa Siqueira,
 Departamento de Física, Universidade Estadual de Ponta Grossa,
 Av. Gen. Carlos Cavalcanti 4748, 84.030-000, Ponta Grossa, Paraná, Brazil

and Maurício Pereira Cantão
 LACTEC, Centro Politécnico da UFPR, 81.531-990, Curitiba, Paraná, Brazil
 Received on 29 September, 2004

We studied the effect of superconducting fluctuations on the electrical conductivity of granular samples of $Y_{1-x}Pr_xBa_2Cu_3O_{7-\delta}$ superconductors, with $x=0.01, 0.03, 0.05, 0.07$ and 0.10 . Samples were prepared by the standard solid-state reaction technique, with two different types of calcination process, in air at 900°C ($x \leq 0.07$) and in vacuum at 850°C ($0.05 \leq x \leq 0.10$). For the samples prepared in air, our results revealed a splitting of the bulk transition, denoted by T_{C1} and T_{C2} , besides the coherence transition. It was observed fluctuation regimes above the highest transition (T_{C1}) and the lowest transition (T_{C2}). For the samples calcinated in vacuum and high concentrations of Pr, changes were observed in the critical region with chemical substitution of the Pr ion for the Y ion. In the regime of approach to the zero resistance state it was observed an occurrence of a coherence transition for all concentrations of praseodymium.

I. INTRODUCTION

It is known that $PrBa_2Cu_3O_{7-\delta}$ is one of the few materials of the $RBa_2Cu_3O_{7-\delta}$ series ($R = Y$ or rare-earth) which supposedly does not superconduct. Although, it was found that $Y_{1-x}Pr_xBa_2Cu_3O_{7-\delta}$ (YPBCO) grown by travelling-solvent floating zone method [1] and in some low-temperature pulsed-laser thin films of Pr-123 [2], exhibits superconductivity. The $PrBa_2Cu_3O_{7-\delta}$ compound is not only non-superconducting, but it is also an antiferromagnetic insulator. From substitution of Y for Pr, the depression of T_C was observed with superconductivity disappearing for $x > 0.55$ [3] and antiferromagnetic ordering of Pr ions with Néel temperature T_N of 17 K at $x=1$.

Some models [4-7] have been proposed to explain the lack of superconductivity in $PrBa_2Cu_3O_{7-\delta}$, including hole-filling, pair breaking, hole localization and percolation models but, in spite of an enormous number of experimental and theoretical investigations the reasons for the quenching of the superconducting state, by intrinsic or extrinsic aspects, is still not well understood. Careful studies of the conductivity could help to reveal the mechanism of nonsuperconductivity in YPBCO. From the measurements of the conductivity and the fluctuation-induced conductivity, it is possible to separate what is fundamentally disorder at microscopic and mesoscopic levels. An important point for the study is the influence of the Pr ion in the fluctuation regimes, especially in the critical regimes.

In this paper, we describe fluctuation conductivity in polycrystalline samples of $Y_{1-x}Pr_xBa_2Cu_3O_{7-\delta}$ ($0 \leq x \leq 0.10$). Samples were prepared by the standard solid-state reaction technique, with two different types of calcination process, air ($x \leq 0.07$) and vacuum ($0.05 \leq x \leq 0.10$). To identify power-law divergences in the conductivity, the results were analyzed with the logarithmic temperature derivative of the conductivity [8]. The content of praseodymium and the different types of calcination process used for sample preparation, produced considerable modifications in the superconducting transition and consequently in the fluctuation regimes.

II. EXPERIMENTAL DETAILS

Polycrystalline samples of $Y_{1-x}Pr_xBa_2Cu_3O_{7-\delta}$ with $x=0.01, 0.03, 0.05, 0.07$ and 0.10 were prepared by the solid-state reaction technique. Appropriate amounts of pure Pr_6O_{11} , $BaCO_3$, CuO and Y_2O_3 were mixed and calcinated in air at 900°C ($x \leq 0.07$) and in vacuum at 850°C ($0.05 \leq x \leq 0.10$) during 18 hours. This process was repeated twice. The product was then pressed into pellets for sintering process at 940°C in air for 24 hours and then slowly cooled through 700°C . Finally, these pellets were then heated in flowing oxygen at 400°C for 48 hours. The lower calcination temperature and the absence of an O_2 -rich atmosphere for $0.05 \leq x \leq 0.10$ were necessary to prevent the formation of Pr_6O_{11} , Ba_2CuO_3 , $PrBa_2O_7$ or other secondary phases [9,10], which tend to form for large x at temperatures above 900°C in the presence of O_2 .

The electrical resistivity, as a function of temperature, was measured by means of a four-probe AC technique at a frequency of 37 Hz. The measuring current was limited to 100 mA for bar-shaped samples approximately $8 \times 3 \times 1.5 \text{ mm}^3$. The temperature was determined by an accuracy of 0.01 K by precisely measuring the resistance of a Pt-100 sensor. With this accuracy data points were so closely spaced, that the temperature derivative of the resistivity, $d\rho/dT$, could be numerically determined in the temperature interval near T_C .

III. RESULTS AND DISCUSSION

A. Method of Analysis for Fluctuation Regimes

Thermal fluctuations create Cooper pairs in superconductors above the critical temperature and, this gives an excess conductivity, also called paraconductivity. We can extract paraconductivity $\Delta\sigma$ assuming that it diverges as power-law given by

$$\Delta\sigma = A\varepsilon^{-\lambda} \quad (1)$$

where $\Delta\sigma = \sigma - \sigma_R$, A is a constant, $\varepsilon = (T - T_C)/T_C$ is the reduced temperature and λ is the critical exponent. From resistivity measurements, $\rho(T)$, we get the conductivity and σ and σ_R , the regular conductivity. In our samples, σ_R is found by linear extrapolation of the resistivity curve in the range $2T_C$ up to room temperature.

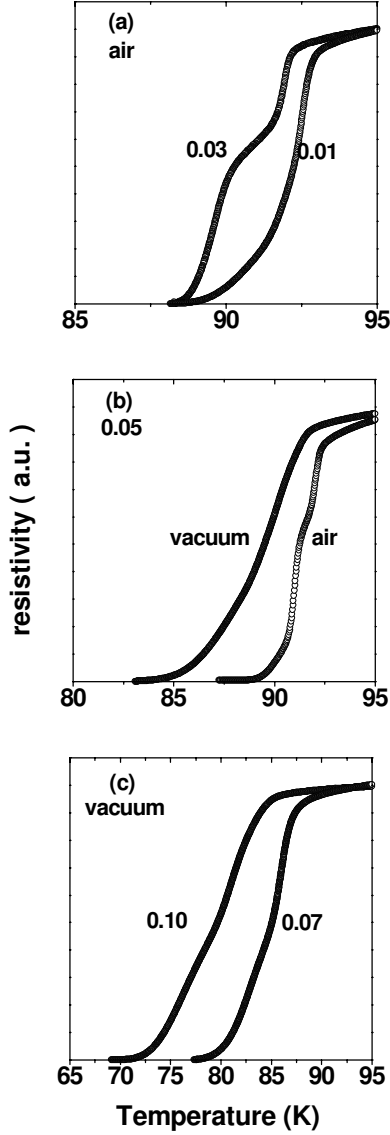


FIG. 1: Electrical resistivity $\rho(T)$ for the series of $Y_{1-x}Pr_xBa_2Cu_3O_{7-\delta}$ ($0.01 \leq x \leq 0.10$) as function of temperature near the critical temperature. The calcination process denominated air and vacuum is discussed in the text. Current density was 200 mA/cm^2 at null field.

To obtain the values for λ and T_C , we determine numerically the logarithmic derivative of $\Delta\sigma$ from experimental data and define

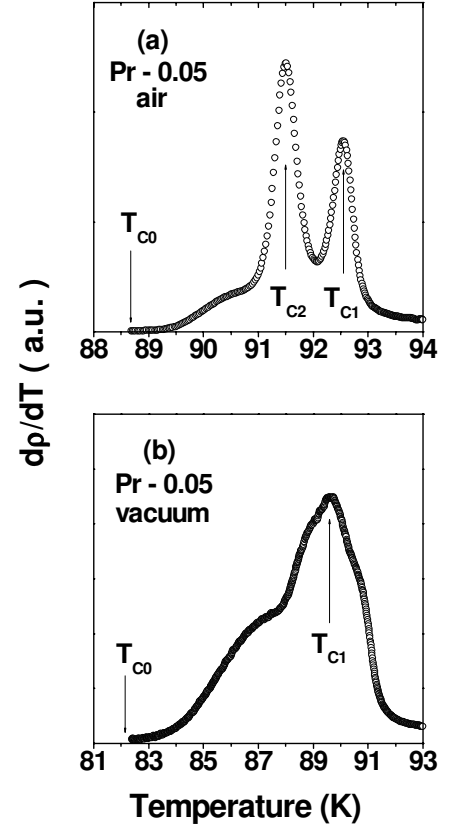


FIG. 2: Temperature derivative of the resistivity $d\rho/dT$ versus temperature for $x = 0.05$ for two different types of calcination process, denominated air and vacuum. T_{C1} and T_{C2} are related to the splitting of the bulk transition and T_{C0} to the coherence transition.

$$\chi_\sigma = -\frac{d}{dT} \ln(\Delta\sigma). \quad (2)$$

Combining Eqs. (1) and (2), we obtain

$$\frac{1}{\chi_\sigma} = \frac{1}{\lambda}(T - T_C). \quad (3)$$

Then, it is possible to determine simultaneously T_C and λ by plotting χ_σ^{-1} versus T [8].

B. Fluctuation Regimes

The resistivity measurements are plotted as function of temperature, around T_C for different degrees of substitution of Pr in $Y_{1-x}Pr_xBa_2Cu_3O_{7-\delta}$ in Fig. 1. The doping with Pr results in the degradation of the superconductivity with a systematic reduction of the midpoint T_C as x clearly increases. The transition widths are for $x < 0.05$ about $\Delta T_C \approx 3 - 4 \text{ K}$ and for

$0.05 \leq x \leq 0.10$ about $\Delta T_C \approx 9 - 20$ K. The results, also indicate that all samples show a metallic-like behavior at high temperatures.

In Fig. 2 the variation of $d\rho/dT$ as function of temperature is shown for samples studied with $x=0.05$ of Pr. The plot of $d\rho/dT$ is a simple procedure for magnifying details of the transition. In this plot it is seen clearly that the transitions are different for air and vacuum processes. In air process, the transition width is approximately 4 K, while in vacuum process the width is about 9 K. Also, our data curves reveal a splitting of the bulk transition [11] for the air but not for the vacuum process. The upper (T_{C1}) and lower (T_{C2}) transitions appear in the temperature derivative as two narrow and prominent peaks. We can also observe in Fig. 2(a) that there is an asymmetry at the temperature region above T_{C0} (between T_{C0} and T_{C2}), as well as, between T_{C0} and T_{C1} for the vacuum process. T_{c0} is a temperature which is close to the so-called zero resistance temperature. A small peak or an asymmetry in $d\rho/dT$ occurs systematically in polycrystalline samples indicating the occurrence of a two-stage intragranular-intergranular transition.

The observation of a splitting pairing transition in $Y_{1-x}Pr_xBa_2Cu_3O_{7-\delta}$ polycrystalline samples was also observed in samples with higher as well as lower concentrations of Pr processed in air. In addition, the two close superconducting transitions were observed in $Y_{0.95}Pr_{0.05}Ba_2Cu_3O_{7-\delta}$ single crystals [11]. For the single crystals, which were observed by electronic microscopy, measurements of resistive transition and magnetic irreversibility the inhomogeneity hypothesis was completely excluded.

Figure 3 shows χ_{σ}^{-1} as a function of T for $x=0.05$ for two different types of calcination process, denominated (a) air and (b) vacuum. In panel (a), we can observe the occurrence of a whole set of fluctuation regimes above the highest transition (T_{C1}) and the lowest transition (T_{C2}). Above T_{C1} we obtain two straight lines with the corresponding exponents $\lambda_{cr} \cong 0.16 \pm 0.02$ and $\lambda_{cr} \cong 0.31 \pm 0.02$, that are fits of χ_{σ}^{-1} to Eq. (3). The first regime was interpreted as precursory of a weak first-order transition [8] and the existence of such regime was first noticed by Pureur *et al.* [12]. The other regime is consistent with 3D-XY model and it had already been observed in polycrystalline and single-crystal samples [8,13,14]. Decreasing the temperature, but above T_{C2} , we observe that χ_{σ}^{-1} shows again another power law regime given by $\lambda_{cr} \cong 0.33 \pm 0.02$. Below T_{C2} and near the zero resistance state the fluctuation conductivity is described by another power law with exponent $s \cong 2.0$, and it is interpreted as being intrinsically related to superconducting granularity from mesoscopic level [15].

In panel (b) we show the results for Pr-0.05 prepared in vacuum. Comparing panel (a) and (b) we can observe considerable modifications in the transition for the different calcination processes, for example, the disappearing of the splitting of the pairing transition. Above T_{C1} (or T_{C2}) two straight lines with the same exponents of the panel (a) can be observed, $\lambda_{cr} \cong 0.16 \pm 0.02$ and $\lambda_{cr} \cong 0.33 \pm 0.02$. Below T_{C1} and above T_{C0} the fluctuation conductivity is described by an-

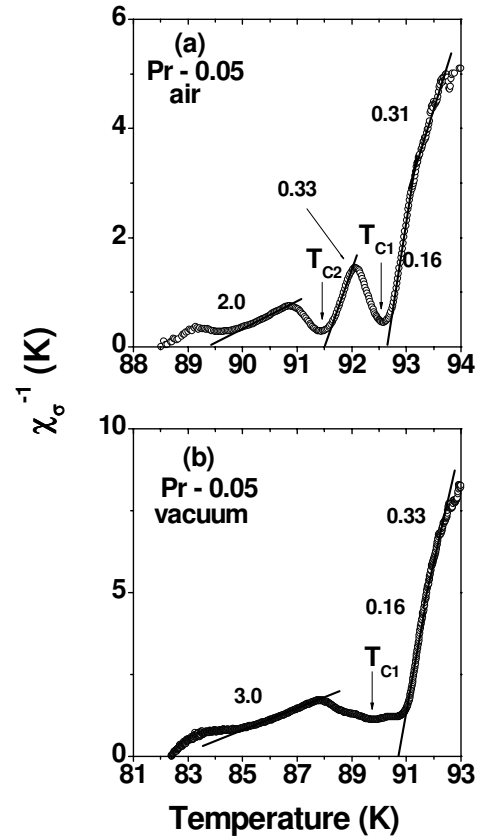


FIG. 3: Panel (a) and (b) represent the inverse of the logarithmic derivative of the conductivity χ_{σ}^{-1} as function of T for $\chi = 0.05$ of Pr, with two different types of calcination process, denominated air and vacuum. The straight lines represent the best fits to the data using Eq. (3), with the quoted exponents.

other power law with exponent $s_1 \cong 3.0$. As expected in a paracoherent-coherent transition, in samples which disorder at mesoscopic level dominate, the fluctuation conductivity near the zero-resistance state must diverge with the exponent considered quite large ($s \cong 3.0$). This transition occurs when the fluctuating phases of the order parameter in individual grains become long-range ordered [15].

In Fig. 4 we show (a) $d\rho/dT$ and (b) χ_{σ}^{-1} as function of temperature around T_{C1} for Pr-0.10 prepared in vacuum. In Fig. (a), we can observe the maximum of $d\rho/dT$ that corresponds approximately to the bulk critical temperature [16]. In panel (b), the temperature range above the maximum of $d\rho/dT$ (T_{C1}), we obtain a fit of χ_{σ}^{-1} which gives the exponent $\lambda \cong 0.40 \pm 0.02$. In the inset of Fig. 4(b), it is shown the same region for Pr-0.07 prepared in vacuum, but with value $\lambda_{cr} \cong 0.33 \pm 0.01$. We clearly observe that the critical regime above T_{C1} depends on the concentration of Pr, with degradation of the regime when x increases from $\lambda_{cr} \cong 0.16 \pm 0.02$ (Pr-0.05) to $\lambda \cong 0.40 \pm 0.02$ (Pr-0.10). The regime corresponding to the exponent $\lambda=0.40$ is interpreted as resulting from almost three-dimensional (3D) Gaussian fluctuations [15]. In the temperature range below the maximum, we can

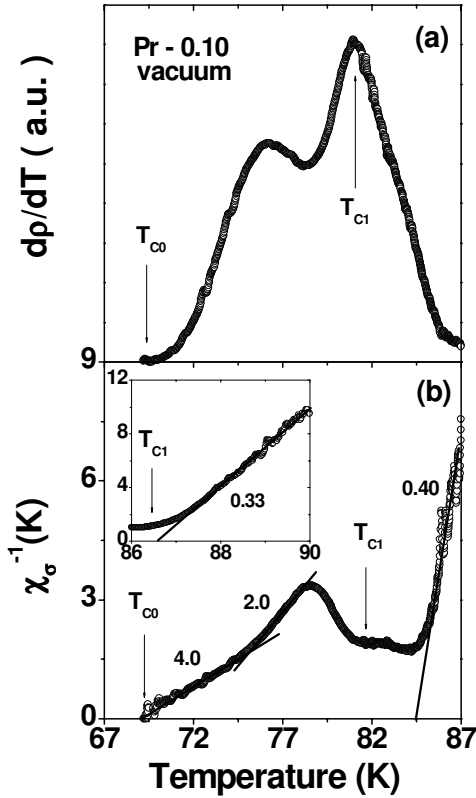


FIG. 4: Plot of (a) dp/dT and (b) $\chi\sigma^{-1}$ as a function of T for $x=0.10$ of Pr calcinated in vacuum. In the inset of panel (b), it is shown $\chi\sigma^{-1}$ as function of T for Pr-0.07 prepared in vacuum. Current density was 180 mA/cm^2 at null field.

see a small peak that is related to the disorder at mesoscopic level. In panel (b) and in the same region, we can observe in large temperature interval power law regimes described by large exponents with values given by $s_1 \cong 4.0 \pm 0.2$ and $s_2 \cong 2.0 \pm 0.2$ characterizing again a phase transition from a paracoherent to a coherent state of the granular array.

From conductivity measurements in polycrystalline samples, in which grain boundaries, Pr_6O_{11} residues, porous and other secondary phases are always present, it was possible to separate the effects due to the granularity from that homogeneous regions marked by the pairing transition. Independently

of the calcination process and content of Pr, the granular character was always present in our samples and important alterations on the power law regimes related to granularity were not observed.

On the other hand, important modifications were observed close to T_{C1} as the suppression of the splitting of the bulk transition and the increase of the value of the exponent above T_{C1} . In the first case, the suppression depended uniquely on the thermal process used during the sample preparation, principally due to the absence of an O_2 -rich atmosphere. Note that the Pr-0.05 (vacuum) sample does not show the two close genuine superconducting transitions while the Pr-0.05 (air) sample does. And for samples prepared in air with $x \geq 0.05$, the same structure was observed. In the second case, we have the increase of the value of the exponent. It can be seen in Figs. 3(a) and (b) that the different calcination processes used during the sample preparation (air and vacuum) did not produce alterations in the value of the critical exponent above T_{C1} , given by $\lambda_{cr} \cong 0.16 \pm 0.02$. This clearly demonstrates that it was the chemical substitution of the Pr ion for the Y ion in the $\text{Y}_{1-x}\text{Pr}_x\text{Ba}_2\text{Cu}_3\text{O}_{7-\delta}$ system that resulted in an increase in the value of the exponent. Such increase, is probably related to the change of the valence state due to the presence of the Pr ion or to the production of defects, most likely Pr on a Ba site.

IV. CONCLUSION

In conclusion, we have studied the excess conductivity of granular samples of $\text{Y}_{1-x}\text{Pr}_x\text{Ba}_2\text{Cu}_3\text{O}_{7-\delta}$ ($0 \leq x \leq 0.10$) superconductors. For samples prepared in air, we observed that our results revealed a splitting of the bulk transition, besides the coherence transition. For the samples prepared in vacuum and with high concentrations of Pr changes were observed in the critical region with the Pr ion destructing the critical regime. In the regime of approach to the zero resistance state we observed the occurrence of coherence transition, independently of the concentration of Pr and of the calcination process.

V. ACKNOWLEDGEMENTS

This work was partially financed by the Conselho Nacional de Pesquisa (CNPq) under contract n° 475347/00-3.

[1] Z. Zou, J. Ye, K. Oka, and Y. Nishihara, Phys. Rev. Lett. **80**, 1074 (1998).
 [2] H. A. Blackstead, J. D. Dow, D. B. Chrisey, J. S. Horwitz, M. A. Black, P. J. McGinn, A. E. Klunzinger, and D. B. Pulling, Phys. Rev. B **54**, 6122 (1996).
 [3] J. J. Neumeier, M. B. Maple, Physica C **191**, 158 (1992).
 [4] J. J. Neumeier, T. Bjornholm, M. P. Maple, and I. K. Schuller, Phys. Rev. B **63**, 2516 (1989).

[5] J. L. Peng, P. Klavins, R. N. Shelton, H. B. Radousky, P. A. Hahn, and L. Bernardez, Phys. Rev. B **40**, 4517 (1989).
 [6] J. Fink, N. Nucker, H. Romberg, M. Alexander, M. B. Maple, J. J. Neumeier, and J. W. Allen, Phys. Rev. B **42**, 4823 (1990).
 [7] C. Infante, M. K. El Mously, R. Dayal, M. Hausain, S. A. Siddiqi, and P. Ganguly, Physica C **167**, 640 (1990).
 [8] P. Pureur, R. M. Costa, P. Rodrigues Jr., J. Schaf, and J. V. Kunzler, Phys. Rev. B **47**, 11420 (1993).

- [9] P. N. Lisboa-Filho, S. M. Zanetti, A. W. Mombrú, P. A. P. Nascente, E. R. Leite, W. A. Ortiz, and F. M. Araújo-Moreira, *Supercond. Sci. Technol.* **14**, 522 (2001).
- [10] A. Kebede, C. S. Jee, J. Schwegler, J. E. Crow, T. Mihalisin, G. H. Myer, R. E. Salomon, P. Schlottmann, M. V. Kurie, S. H. Bloom, and R. P. Guertin, *Phys. Rev. B* **40**, 4453 (1989).
- [11] F. M. Barros, V. N. Vieira, F. W. Fabris, M. P. Cantão, A. R. Jurelo, P. Pureur, and J. Schaf, submitted for publication.
- [12] W. Holm, Yu. Eltsev, Ö. Rapp, *Phys. Rev. B* **51**, 11992 (1995).
- [13] J. R. Rojas, A. R. Jurelo, R. M. Costa, L. M. Ferreira, P. Pureur, M. T. D. Orlando, P. Prieto, and G. Nieva, *Physica C* **341-348**, 1911 (2000).
- [14] P. Pureur, R. Menegotto Costa, *Fluctuation Phenomena in High Temperature Superconductors*, in: Ausloos, A. A. Varlamov (Eds.), NATO ASI Series, Vol. 32, Kluwer Academic Publishers, Dordrecht, 1997, p. 259.
- [15] A. R. Jurelo, J. V. Kunzler, J. Schaf, P. Pureur, J. Rosenblatt, *Phys. Rev. B* **56**, 14815 (1997), A. R. Jurelo, I. Abrego Castillo, J. Roa-Rojas, L. M. Ferreira, L. Ghivelder, P. Pureur, and P. Rodrigues Jr., *Physica C* **311**, 133 (1999).
- [16] M. Auloos, Ch. Laurent, *Phys. Rev. B* **37**, 611 (1988).